## General Comments:

**Reviewer:** *This is an excellent paper... I recommend this manuscript for publication after my comments/suggestions below have been taken into account by the authors.*

**Response:** We sincerely thank the reviewer for the highly positive assessment and constructive feedback. We are particularly encouraged that the reviewer recognises the value and thoroughness of our automated grounded iceberg detection algorithm. Below, we address each comment point-by-point and outline the specific changes we will make in the revised manuscript.

## Specific Comments:

**Comment 1:** *Page 2 line 21: "picket fence effect" related to which process?*

**Response:** We thank the reviewer for pointing this out. The "picket fence effect" refers to the process where high-density clusters of grounded icebergs act as a series of physical anchors that stabilise landfast sea ice and restrict its drift and export. Since this term first appears in the Abstract, in the revision we will add a brief clarifying phrase directly in the Abstract (e.g., "acting as physical anchors to stabilise fast ice") to ensure immediate clarity. The detailed physical mechanism of this effect will be further elaborated in our Result (Section 4.2.2).

**Comment 2:** *Page 3 lines 45-48: I do not see the immediate relation between obstruction of sea ice export on the one hand and the formation of a coastal latent heat polynya... Is it possible to add a SHORT explanation?*

**Response:** We appreciate the opportunity to clarify this mechanism. The formation of a latent heat polynya requires winds to blow ice away from the coast or another barrier (e.g., fast ice, grounded bergs, glacier tongues). Grounded icebergs can act as topographic barriers that impede the advection of sea ice from (generally) east to west in the westward Antarctic Coastal Current (Massom et al., 2001; Fraser et al., 2023). This blocking effect prevents external pack ice from drifting into the polynya area, allowing offshore winds to clear the downstream (leeward) side of the icebergs, i.e., the polynya area, thereby sustaining the polynya (e.g., see the conceptual schematic in Figure 11 of Fraser et al., 2023; Ohshima et al., 2013). In the revised manuscript, we will add a short, intuitive explanation to clarify this dynamic.

**Comment 3 & 4**: *Page 6 lines 133-136: Pixel size... Which product was used: GRD-HR or GRD-MR?... EWS stronger detection than IWS?... ENL issues... Default values for pyroSAR?*

**Response:** We thank the reviewer for the detailed technical questions regarding the Sentinel-1 SAR products and processing parameters.

Regarding the processing details, we would like to clarify that the original manuscript contained an error where the IW mode data were mistakenly described as GRD products. Upon a thorough review of our data workflow, we confirmed that we utilized GRD-MR products for the EW mode (197 scenes) and Single Look Complex (SLC) products for the IW mode (77 scenes).

During this data verification process, we discovered that 15 out of the 77 IW scenes had inadvertently been processed as GRD data in our earlier iteration. To maintain strict methodological consistency across the entire study, we have re-acquired the original SLC files for these 15 scenes, re-run them through our dedicated IW processing pipeline, and updated the circum-Antarctic dataset. Consequently, we will thoroughly modify the Data Section of the manuscript to accurately reflect these data types, software packages, and workflows. As a result of updating these 15 scenes, some numerical values and statistics in the results section have been slightly adjusted in the revised manuscript. We emphasize that these changes are minor and have no material impact on the overall trends, model performance, or conclusions of our study.

To fully answer your specific questions regarding the product parameters and the Equivalent Number of Looks (ENL):

- **EW GRDM Data:** The original EW GRDM product is distributed with 40 m pixel spacing and a nominal ENL of 10.7 (approximately 6 x 2 looks in range and azimuth, see Table below with the specifications from ESA). We did not apply any additional multi-looking during pre-processing.
- **IW SLC Data:** Rather than using ESA’s standard IW GRD products (with nominal ENLs of 4.4 or 81.8 for GRDH and GRDM), we processed the SLC data (nominal ENL = 1) directly to a 20 m pixel spacing Radiometric Terrain Corrected (RTC) product. This was undertaken using the Geoscience Australia *sar-pipeline*, which implements the NASA JPL RTC and ISCE3 software packages. The ISCE3 software applies adaptive multi-looking to achieve the 20 m pixel spacing. This adaptive approach results in a spatially varying ENL based on local terrain, yielding an approximate scene-level ENL of ~16 (estimated from resampling the nominal ~2.3 × 14.1 m pixel spacing to 20 × 20 m).

  We will add the correct and detailed description of both EW GRDM and IW SLC processing to the manuscript, including the following paragraph that summarizes the most important information:

“In summary, the final gamma-nought intensity images obtained after pre-processing exhibit comparable visual characteristics for both EW and IW acquisition modes. However, IW images feature half the pixel spacing and slightly higher ENL compared to EW images. These differences stem from the intrinsic properties of the respective acquisition modes, where EW prioritizes broader spatial coverage at the expense of spatial and/or radiometric resolution.”

For your convenience and reference, we have also attached the table outlining the Sentinel-1 product specifications to this response.

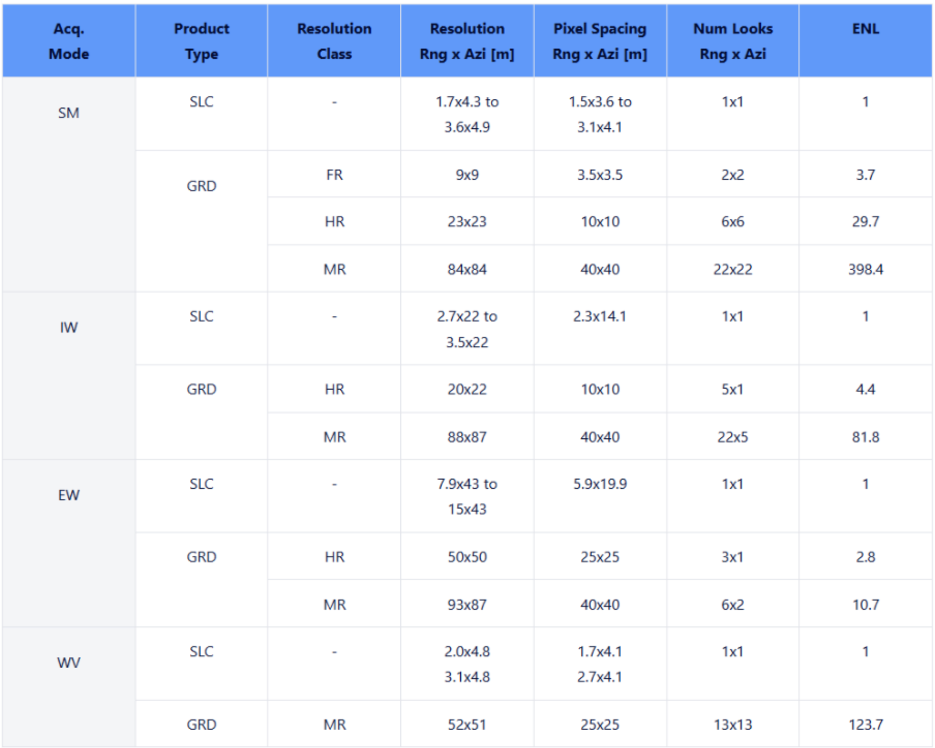

| Acq. Mode | Product Type | Resolution Class | Resolution Rng x Azi [m] | Pixel Spacing Rng x Azi [m] | Num Looks Rng x Azi | ENL |
|---|---|---|---|---|---|---|
| SM | SLC | - | 1.7x4.3 to 3.6x4.9 | 1.5x3.6 to 3.1x4.1 | 1x1 | 1 |
| | GRD | FR | 9x9 | 3.5x3.5 | 2x2 | 3.7 |
| | | HR | 23x23 | 10x10 | 6x6 | 29.7 |
| | | MR | 84x84 | 40x40 | 22x22 | 398.4 |
| IW | SLC | - | 2.7x22 to 3.5x22 | 2.3x14.1 | 1x1 | 1 |
| | GRD | HR | 20x22 | 10x10 | 5x1 | 4.4 |
| | | MR | 88x87 | 40x40 | 22x5 | 81.8 |
| EW | SLC | - | 7.9x43 to 15x43 | 5.9x19.9 | 1x1 | 1 |
| | GRD | HR | 50x50 | 25x25 | 3x1 | 2.8 |
| | | MR | 93x87 | 40x40 | 6x2 | 10.7 |
| WV | SLC | - | 2.0x4.8<br>3.1x4.8 | 1.7x4.1<br>2.7x4.1 | 1x1 | 1 |
| | GRD | MR | 52x51 | 25x25 | 13x13 | 123.7 |

Regarding the observation that the EW mode exhibits stronger detection capability than the IW mode, we agree with the reviewer that a higher ENL should intuitively increase detection performance. However, in our specific application, this discrepancy is primarily driven by data availability and model training rather than the inherent physics of the SAR modes. First, the EW data available for our study primarily consisted of cross-polarisation (HV), whereas the IW data were largely restricted to co-polarisation (HH). As cross-polarisation provides a significantly higher backscatter contrast between icebergs and surrounding sea ice compared to co-polarisation, the model naturally achieved better segmentation performance on the EW (HV) imagery. Second, our deep learning model was trained on a dataset predominantly composed of EW imagery, making the network inherently more attuned to the feature representations of EW data. In the revised manuscript, we will add a brief discussion to clarify these specific reasons.

**Comment 5:** *Page 7 Fig 1: Only one region was used for validation... Was this region chosen because of optimal availability...? Would you expect similar results in other regions?*

**Response:** We thank the reviewer for this important question. To clarify, the Adélie Land region was selected for the full-year, cross-seasonal validation not due to a lack of data elsewhere, but because it presents a highly complex and representative environmental background throughout the year. This region consistently features a challenging mix of open water, landfast sea ice, and fragmented pack ice, making it a rigorous testbed for assessing seasonal variations such as summer melt.

Regarding other regions, we indeed expect similar results across the Antarctic margin. For the specific temporal window of our dataset (February–April), we have already demonstrated the algorithm's spatial generalisation across multiple other distinct coastal regions (e.g., Princess Ragnhild Coast, Princess Martha Coast), as detailed in Section 3.5.1 and Table 5.

In terms of cross-seasonal performance, performance drops are generally as expected during the summer surface melt season, or under specific extreme conditions, such as severe wind-driven sea clutter (mainly in IWS mode, co-polarisation) or within heavily deformed sea ice rubble, where the inherent radar contrast between icebergs and the background is highly reduced. Because these factors are not unique to Adélie Land, we would expect the model to maintain a similar level of year-round stability across other regions, provided those specific extreme conditions are not present.

**Comment 6:** *Page 10, section 3.1.3: I suggest to mention here the possible combinations of the image pairs... and whether image sequences ≥ 3 are used.*

**Response:** We thank the reviewer for pointing this out. We realise that while the overall data combinations are mapped in Figure 1, the specific combinations used during the multi-temporal matching process could be stated more explicitly.

Because our tracking framework analyses repeat-pass imagery along the same orbital track, the image pairs used for cross-temporal matching within any given trajectory almost exclusively consist of the *same* acquisition mode and polarisation (e.g., matching EW-HV to EW-HV, or IW-HH to IW-HH). While our algorithm operates on extracted shapes and could theoretically match targets across different modes in spatially overlapping areas, cross-mode matching does not occur in our dataset. We specifically opted for this approach because maintaining a consistent 12-day temporal resolution is highly beneficial for overall data consistency. A 12-day repeat cycle is already sufficient for identifying long-term stationary targets; inserting additional detections from different modes or polarisations to create mixed sequences would disrupt this temporal consistency without adding significant practical benefit to our grounded iceberg identification.

In the revised manuscript, we will add a brief sentence to Section 3.1.3 clarifying both that the matching pairs are typically consistent in mode/polarisation, and that continuous image sequences ($n \geq 3$) are utilised.

**Comment 7 & 8:** *Page 11 & 12: Thresholds and training parameters: Are they based on own experiments or literature? Sensitivity? How many training sessions?*

**Response:** We thank the reviewer for raising these important questions. As these parameters govern different stages of our pipeline, we address them categorically below:

1. Deep Learning Training Parameters:

The training hyperparameters (such as learning rate, batch size, and weight decay) were determined through our own experiments using Bayesian optimisation to balance model convergence and segmentation accuracy. In the revision, we will state the total number of training sessions conducted. In total, approximately 50 independent training sessions were conducted during model development and hyperparameter optimisation.

2. Grounded Iceberg Identification Algorithm Thresholds (Page 15):

The matching thresholds (e.g., centroid distance of 10 pixels, area difference of 0.5, and Intersection over Union (IoU) limits) are empirical, derived through careful tuning and extensive visual inspection of our identification results.

Rather than conducting a strictly quantifiable sensitivity analysis—which is challenging given the immense variability in iceberg sizes, grounding behaviours (e.g., completely stationary versus rotating in place), and high-density spatial clustering (where densely packed targets frequently merge during segmentation, as illustrated in Supplementary Figures S1 and S4)—we focused on establishing a geometrically sound balance.

For instance, the centroid distance threshold required careful consideration: a value that is too large risks incorporating slow-drifting icebergs into stationary trajectories (increasing false positives), while a value that is too strict would prematurely break trajectories due to minor spatial shifts caused by iceberg tilting or rotation. Similarly, the area and IoU thresholds were determined empirically; the inherent instability in segmenting dense, clustered icebergs and the morphological variations across different time steps necessitated these specific values to ensure robust, continuous matching.

Furthermore, the inherent complexity of certain regional environments limits the effectiveness of generic threshold tuning. For example, in regions characterised by an exceptionally high density of small, mobile icebergs, such as the Bellingshausen Sea, we observed a specific type of false positive. Despite the robust performance of both the detection model and the tracking algorithm, in some cases these may have been misidentified as grounded when small, “similarly shaped” drifting bergs coincidently occupied overlapping positions between consecutive 12-day SAR passes. Because these coincidental overlaps perfectly satisfy the algorithm's temporal continuity and spatial constraints (e.g., IoU and centroid distance), no simple threshold adjustment can completely eliminate them without simultaneously breaking the retrieval of genuinely grounded targets. We will add a clarification in Section 5.2 (Limitations) of the manuscript.

3. Physical Constraint Filters (Table 2):

As briefly stated in Section 3.4, the post-processing filters are based on a combination of established literature and our empirical observations. The bathymetric limits (e.g., > 1000 m excluding grounding entirely) are grounded in the literature regarding maximum expected keel depths for Antarctic icebergs (e.g., Dowdeswell and Bamber, 2007). The combined thresholds of Area and Sea Ice Concentration (SIC) in shallower waters (< 600m) were empirically determined by observing the radiometric behaviour of sea-ice rubble. As detailed in Section 5.2 and quantified in Table 7, this approach is physically justified and necessary to balance accuracy: it effectively filters out a significant volume of smaller sea-ice artefacts (e.g., removing over 3,500 targets in shallow waters) while safely retaining larger, deep-keeled icebergs.

**Comment 9:** *Page 13, line 260: The term “trajectory reconstruction” irritated me at first sight … section 3.3.2 where a detailed explanation is given.*

**Response:** We agree with the reviewer that the term "trajectory reconstruction" can incorrectly imply drifting motion. To prevent any reader confusion, we will change this terminology to "stationary target identification" in the revision. Furthermore, we will include a direct cross-reference to Section 3.3.2, where the detailed explanation of the stationarity test is provided.

**Comment 10:** *Page 16, section 3.4: The criteria for excluding icebergs dependent on SIC and water depth trigger the following comments: (a) It may be possible that the SIC data and/or seabed topography data are not accurate... Its exclusion means that I get a false negative. (b) A hint of typical keel depths of Antarctic icebergs would be helpful.*

**Response:** We thank the reviewer for these insightful points.

(a) We acknowledge that inaccuracies or coarse spatial resolutions in the underlying auxiliary datasets (such as IBCSO bathymetry or AMSR2 SIC) could theoretically lead to the erroneous exclusion of a truly stationary, grounded iceberg, thereby creating a false negative. In the revised manuscript, we will add a sentence to the Discussion (Section 5.2) explicitly noting this inherent limitation of utilising auxiliary filtering datasets.

(b) We appreciate this suggestion. As briefly noted in our Introduction (lines 31–32), Antarctic icebergs retain substantial subsurface drafts typically spanning from tens of metres to depths exceeding 500 metres (Dowdeswell and Bamber, 2007). To ensure this context is readily available when discussing our filtering criteria (Table 7), we will add a brief cross-reference in Section 3.4 reminding the reader of these typical keel depths, thereby explicitly linking this literature to the physical justification for our specific bathymetric thresholds. In addition to a hint of keel depths estimated from surface elevation of ice shelves' marine margins, we will add "As reported by Luckman et al. (2010), nine grounded icebergs in the western Weddell Sea have maximum grounding depths estimated from satellite altimetry ranging from 240 - 370 m."

**Comment 11:** *Page 24, line 510: “Table 7” in parentheses?*

**Response:** We thank the reviewer for catching this oversight. We will correct this formatting error.

**Comment 12:** *Page 24, Table 6: In the caption for the table, it could be made clear that here sequences of n images are analysed and “start” and end” refer to the image number in the sequence at which an iceberg was first and last identified as stationary by the algorithm. Or point to section 4.1.2.*

**Response:** We thank the reviewer for the valuable suggestion. We will update the caption of Table 6 in the revision to explicitly define the "start" and "end" terminology in the context of the analysed image sequences, and we will add a pointer to Section 4.1.2 for further clarity.

**Comment 13:** *Page 29, line 567: ice(Fraser. => missing space*

**Response:** We thank the reviewer for catching this oversight. We will correct this typographical error in the revised manuscript.

**Comment 14:** *Page 31, line 634: do you really mean areas with complex "fast-ice topography" and not "seabed topography"?*

**Response:** Yes, we specifically meant "fast-ice topography". Complex and heavily deformed fast-ice surfaces (such as pressure ridges and rubble fields) can produce strong radar backscatter signals that closely mimic the radiometric signatures of small icebergs.

**Comment 15:** *Page 32, section "Future Work": (a) I am sceptical regarding the mentioned merits of altimetry... (b) Multi-source image analysis includes different types of sensors... If you have already an idea what an optimal multi-source scenario could be, you should mention it. (c) Not clear to me: what is the "global contextual information"? How does the knowledge of distant conditions really help to improve detection of a single iceberg in its local environment?*

**Response:** We thank the reviewer for these constructive prompts to expand our Future Work section.

(a) Altimetry: We agree with the reviewer's scepticism to some extent. The reviewer is correct that altimetry (such as ICESat-2) only provides narrow surface elevation profiles. Relying on these sparse profiles is insufficient to fully reconstruct the 3D morphology of individual icebergs, as the satellite ground tracks may only capture a narrow slice or miss tiny targets entirely. Our initial phrasing in Section 5.3 was admittedly overly optimistic regarding "accurate reconstruction of iceberg morphology" for single icebergs. For single-iceberg 3D reconstruction, field-based observations utilising digital elevation models alongside multibeam echosounders remain irreplaceable to capture the complete above- and below-water geometry. However, combining SAR-derived 2D surface areas with altimetry-derived draft/freeboard estimations (where tracks do successfully intersect targets) remains a valuable approach for statistical volume approximation and draft estimation (e.g. Luckman et al., 2010).
Furthermore, these limitations are poised to be mitigated by next-generation missions. Specifically, the proposed Earth Dynamics Geodetic Explorer (EDGE) satellite, targeted for the early 2030s, will employ swath mapping laser altimetry using 40 simultaneous beams to create contiguous, high-density coverage (Garvin et al., 2026). This technological leap will vastly improve spatial sampling resolution, potentially overcoming current observational gaps to enable true 3D morphological reconstructions even for smaller icebergs.
In the revision, we will temper our claims in Section 5.3, clarifying that while full 3D morphological reconstruction is challenging for smaller targets, altimetry primarily facilitates critical draft and volume estimations when fused with 2D SAR boundaries. We will also highlight future swath-mapping altimeters like EDGE as a promising avenue for 3D surface morphology reconstruction.

(b) Multi-source scenario: The reviewer raises an excellent point. While we generally mentioned "multi-source data fusion" in Section 5.3, explicitly defining an optimal scenario will significantly strengthen this section. An optimal multi-source tracking and volume-estimation scenario would integrate high-resolution optical imagery (e.g., Sentinel-2) to cross-validate and compensate for SAR's signal degradation during the summer surface melt season, alongside multi-frequency SAR (e.g., combining our C-band Sentinel-1 baseline with L-band sensors, such as Rose-L) to maximise iceberg-to-sea-ice contrast under complex conditions. In the revision, we will explicitly include these specific sensor and frequency combinations as concrete examples of the optimal multi-source approach.

(c) Global contextual information: By "global contextual information", we refer to the broader spatial context beyond the standard 250 X 250 pixel sub-image tile input to the model. As discussed in Sections 5.2 and 5.3, incorporating this wider view serves two critical purposes. First, it allows the model to perceive the continuous geometry of giant icebergs that span across multiple tiles, thereby preventing fragmented segmentation. Second, integrating a wider spatial context provides richer environmental constraints; this broader perspective helps the model accurately recognise large-scale background interference—such as extensive patches of severe sea clutter or heavily deformed residual fast ice—allowing it to better distinguish true targets from false positive signals. In the revised manuscript, we will rewrite this sentence to explicitly define what we mean by "global contextual information" and detail these two specific benefits.

## References:

Dowdeswell, J. A., & Bamber, J. L. (2007). Keel depths of modern Antarctic icebergs and implications for sea-floor scouring in the geological record. Marine Geology, 243(1-4), 120-131. doi: https://doi.org/10.1016/j.margeo.2007.04.008

Fraser, A. D., Wongpan, P., Langhorne, P. J., Klekociuk, A. R., Kusahara, K., Lannuzel, D., ... & Wienecke, B. (2023). Antarctic landfast sea ice: A review of its physics, biogeochemistry and ecology. Reviews of Geophysics, 61(2), e2022RG000770. doi: https://doi.org/10.1029/2022RG000770

Garvin, J. B., McDonagh-Smith, P., Peters, R. M., Fricker, H. A., Armston, J. D., Blair, J. B., & Luthcke, S. B. (2026). Return on investment and economic impact of a NASA-funded swath mapping laser altimeter orbiter for Earth surface elevations situational awareness in 2031–2040. New Space, 21680256261434504. doi: https://doi.org/10.1177/21680256261434504

Luckman, A., Padman, L., & Jansen, D. (2010). Persistent iceberg groundings in the western Weddell Sea, Antarctica. Remote Sensing of Environment, 114(2), 385-391. doi: 10.1016/j.rse.2009.09.009

Massom, R. A., Hill, K. L., Lytle, V. I., Worby, A. P., Paget, M. J., & Allison, I. (2001). Effects of regional fast-ice and iceberg distributions on the behaviour of the Mertz Glacier polynya, East Antarctica. Annals of Glaciology, 33, 391-398. doi:10.3189/172756401781818518

Ohshima, K. I., Fukamachi, Y., Williams, G. D., Nihashi, S., Roquet, F., Kitade, Y., ... & Wakatsuchi, M. (2013). Antarctic Bottom Water production by intense sea-ice formation in the Cape Darnley polynya. Nature Geoscience, 6(3), 235-240. doi: https://doi.org/10.1038/ngeo1738